

# Vibrational spectra of silicon implanted polymethyl-methacrylate (PMMA) and poly-propylene (PP)\*

M. BALEVA, G. ZLATEVA<sup>a</sup>, T. TSVETKOVA<sup>b\*</sup>, S. BALABANOV<sup>b</sup>, L. BISCHOFF<sup>c</sup>

*Faculty of Physics, Sofia University, 5 J.Boucher Str., 1164 Sofia, Bulgaria*

*<sup>a</sup>Faculty of Medicine, Sofia University, 1 Koziak Str., 1407 Sofia, Bulgaria*

*<sup>b</sup>Institute of Solid State Physics, 72 Tzarigradsko Chaussee, 1784 Sofia, Bulgaria*

*<sup>c</sup>Forschungszentrum Dresden-Rossendorf e.V., P.O.Box 510119, D-01314 Dresden, Germany*

Infra-red (IR) and Raman spectroscopy studies were used to characterize different polymer materials implanted with low energy Si<sup>+</sup> ions ( $E = 30 \text{ keV}$ ,  $D = 1 \cdot 10^{17} \text{ cm}^{-2}$ ). Two kinds of polymer were studied – poly-methyl-methacrylate (PMMA), and poly-propylene (PP). Silicon ion implantation resulted in the breaking down of bonds in the substrate structures, and the emergence of newly formed bonds. The IR and Raman studies thus show that the implantation of Si<sup>+</sup> into PMMA and PP leads to the formation of amorphous and nano-crystalline graphite, predominantly in the PP samples. The presence of SiC particles and unreacted Si atoms is also observed in the implanted polymer material.

(Received November 5, 2008; accepted December 15, 2008)

*Keywords:* Polymers, Ion implantation, Vibrational spectroscopy

## 1. Introduction

In recent years, the growing interest in the ion implantation technique as a tool for the material properties modification of polymers is due to the possibility for precise control of the technological parameters, both for fundamental research purposes and when considering possible applications to device fabrication. The optical, electrical, mechanical and chemical properties can be selectively modified using ion bombardment [1].

The understanding of the structural re-arrangement effects on the relevant optical properties of ion-bombarded polymer surfaces reveals new approaches to the design of devices with desired parameters, e.g. for applications of high-performance polymers for optical filters, absorbers, reflectors, luminescent devices, etc. [2]. This knowledge is of considerable importance for the application of the techniques of ion beam synthesis (IBS) to produce new compounds and advanced materials in irradiated polymer surfaces, by implanting ions of various chemical elements [3-5]. The optical and photoluminescence properties of ion implanted polymers, being of particular interest for modern optoelectronics and photonics, have been extensively explored [6-10].

The aim of the present work was to apply the ion beam technique to produce polymer materials yielding

interesting luminescence properties [9,10] and to study the relevant ion beam modification effects on the structure and chemical bonding arrangements using infra-red (IR) and Raman spectroscopy.

## 2. Experimental

Polymethyl-methacrylate (PMMA) and poly-propylene (PP) samples, commercially available as bulk samples with thicknesses of 2 mm and shaped as squares (sides of 10 mm) or circles (diameters of 10 mm), were studied in the present work.

A Danfysik 1090 ion implanter was used for Si<sup>+</sup> implantation at room temperature (RT). The implantation was carried out at relatively low energies ( $E = 30 - 50 \text{ keV}$ ) and a wide range of ion doses ( $D = 10^{13} - 10^{17} \text{ cm}^{-2}$ ). The beam current was kept under  $2 \mu\text{A}/\text{cm}^2$  during the implantation process, to maintain the target temperature below  $80^\circ\text{C}$  – the temperature at which the polymer material starts to decompose. A high vacuum (of the order of  $10^{-6} \text{ Pa}$ ) was maintained in the target chamber during implantation.

The room temperature infrared transmittance spectra were measured in the range  $500 \text{ to } 2000 \text{ cm}^{-1}$ , using a UR-20 double-beam spectrometer.

\* Paper presented at the International School on Condensed Matter Physics, Varna, Bulgaria, September 2008

The Raman spectra were taken at room temperature using a SPEX 1403 spectrometer equipped with a photomultiplier working in a photon counting mode and with a spectral resolution of  $4\text{ cm}^{-1}$ . The  $488\text{ nm}$   $\text{Ar}^+$  laser line with a power as low as  $10\text{ mW}$  because the thermal stability of the PMMA was only  $65^\circ\text{C}$ .

### 3. Results

#### 3.1 Infrared spectra

The IR spectra of the unimplanted and  $\text{Si}^+$  implanted, at a dose of  $D_3=1.10^{17}\text{ cm}^{-2}$ , polymethyl-methacrylate (PMMA) substrates are compared in Fig. 1. As seen, the absorption of the implanted sample is higher and some features, though not intense because of the small thickness of the modified region, can be resolved.

The IR spectra of the unimplanted and implanted with three different doses,  $D_1=1.10^{16}\text{ cm}^{-2}$  (s.1),  $D_2=3.10^{16}\text{ cm}^{-2}$  (s.2), and  $D_3=1.10^{17}\text{ cm}^{-2}$  (s.3), PP substrates are shown in Fig. 2. The spectra are displayed in the region from  $800$  to  $2000\text{ cm}^{-1}$ , since in the range from  $500$  to  $800\text{ cm}^{-1}$  they are highly transparent. The features in these spectra are much strongly pronounced and the absorption is comparatively higher. The behaviour of the samples, implanted with the three different doses, is similar.

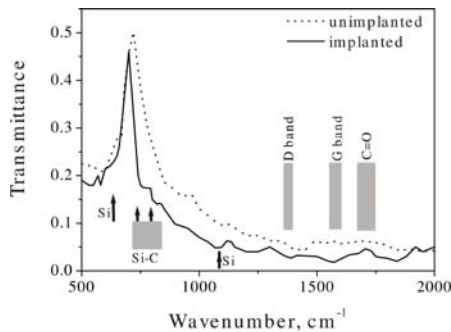


Fig. 1. IR spectra of the unimplanted and  $\text{Si}^+$  implanted at  $D_3=1.10^{17}\text{ cm}^{-2}$  PMMA samples.

#### 3.2 Raman spectra

In Fig. 3, the Raman spectra of the unimplanted and implanted with  $D_3=1.10^{17}\text{ cm}^{-2}$  PMMA substrates are shown, in the range from  $200$  to  $2000\text{ cm}^{-1}$ . The Raman spectra of the unimplanted and implanted with  $D_1=1.10^{16}\text{ cm}^{-2}$  (s.1) and  $D_3=1.10^{17}\text{ cm}^{-2}$  (s.3) PP substrates are shown in Fig. 4, in the wave-number region from  $500$  to  $2000\text{ cm}^{-1}$ .

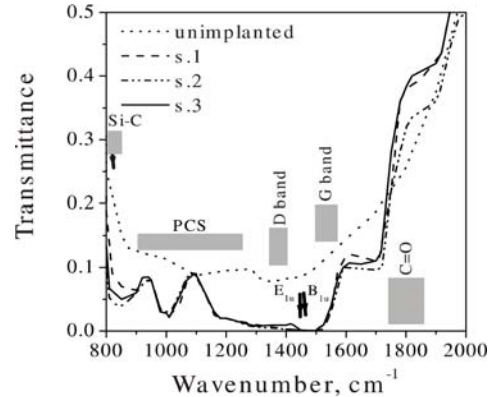


Fig. 2. IR spectra of the unimplanted and  $\text{Si}^+$  implanted at  $D_1=1.10^{16}\text{ cm}^{-2}$  (s.1),  $D_2=3.10^{16}\text{ cm}^{-2}$  (s.2), and  $D_3=1.10^{17}\text{ cm}^{-2}$  (s.3) PP samples.

Because of the low scattering volume of the implanted regions, no significant difference between the spectra of unimplanted and implanted samples is seen. The only unambiguous statement concerns the increase in the scattered light intensity in the range close to  $1550\text{ cm}^{-1}$ , shadowed in Fig. 3. The subtraction of the unimplanted sample spectra from those of the implanted ones gave the spectra, displayed in the insets in Fig. 3 and Fig. 4. It is seen that the difference in the spectra is governed by a broad band peaked at about  $1550\text{ cm}^{-1}$ , as it concerns the samples implanted with the highest doses.

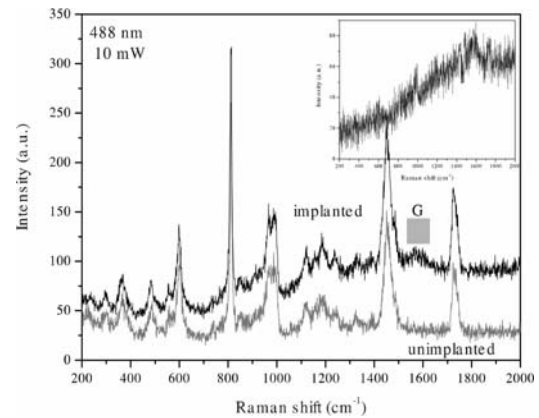


Fig. 3. Raman spectra of the unimplanted and  $\text{Si}^+$  implanted at  $D_3=1.10^{17}\text{ cm}^{-2}$  PMMA samples.

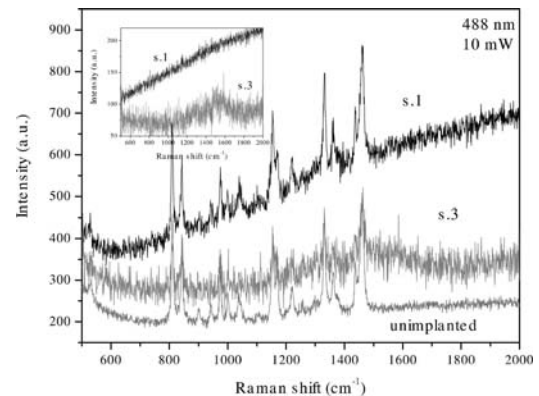


Fig. 4. Raman spectra of the unimplanted and Si<sup>+</sup> implanted at  $D_1=1.10^{16} \text{ cm}^{-2}(\text{s.1})$  and  $D_3 = 1.10^{17} \text{ cm}^{-2}(\text{s.3})$  PP samples.

#### 4. Discussion

After the implantation, both types of the glassy substrates change their colour to a brown-yellow one. The brown-yellow colour of the implanted sample indicates the formation of substances with a high absorption coefficient in the visible range. Taking into account the substrate's structure it is reasonable to expect the presence of graphite-like bonds, SiC nano-crystallites, and unreacted Si atoms in the sample implanted with Si. The formation of new bonds requires the break down of bonds in the substrate structures.

The transparency in the infrared transmittance spectra of the implanted PP substrates (Fig. 2) increases significantly with an increase of the implanted doses in the range 1700 - 1850  $\text{cm}^{-1}$ . The spectrum of the implanted PMMA substrate is also more transparent in the range 1700 - 1750  $\text{cm}^{-1}$ . Stretching vibrations of the C=O bonds at 1720  $\text{cm}^{-1}$  and 1780  $\text{cm}^{-1}$  [11] are reported for polyimide layers. Then, the transparency increase of our samples around these frequencies can reasonably be attributed to the breaking of C=O bonds.

**Graphitic bonds.** The only unambiguous statement, as it concerns the formation of new bonds in both types of substrate, is the presence of C=C bonds. It is confirmed by the IR transmittance, as well as by the Raman spectra. The formation of graphite-like and carbon-rich amorphous structures results in the appearance of broad absorption bands in the infrared spectrum at about 1350  $\text{cm}^{-1}$  and at about 1550  $\text{cm}^{-1}$ , known as D (disorder) and G (graphite) bands, respectively. The bands are usually assigned to the graphitic  $sp^2$  hybridized C bonds. The G band corresponds to vibrations in the graphitic micro-particles and the D band to in-plane vibrational modes at the particle surface [12]. The experimental transmittance spectra displayed in Fig. 1 and Fig. 2 show unambiguously an increase of the absorption of the implanted samples in the range 1300 and 1550  $\text{cm}^{-1}$ , which is an indication of the presence of amorphous and microcrystalline graphite. It is seen, from the insets in Fig. 3 and Fig. 4, that the difference in the Raman spectra of implanted with the highest doses and unimplanted samples is governed by a broad band peaked at about 1550  $\text{cm}^{-1}$ . These spectra look like the spectrum of a network with graphitic  $sp^2$  hybridized C bonds, see for example [13].

The Raman spectrum of single crystal graphite exhibits a single line ( $E_g$  mode) at 1581  $\text{cm}^{-1}$ . A breakdown of the Raman selection rules allows the  $A_{1g}$  mode near 1360  $\text{cm}^{-1}$  to become Raman (and also infrared) active in amorphous and nano-crystalline graphite. Doyle and Dennison [14] consider the graphitic carbon clusters as a continuum random network (CRN) where rings of cluster vibrations cannot be decoupled from the network in which they are embedded. According to these considerations, the in-plane vibrational modes of  $n=4, 5,$

6, 7 and 8 membered symmetric, planar carbon rings with various frequencies  $\omega$  are determined. The interpretation of the Raman spectra of graphitic amorphous carbon [14] leads to the conclusion that the spectra comprise: i. about 20%  $n=5$  ( $E_2$  mode with  $\omega=1100$  and 1529  $\text{cm}^{-1}$ ); ii. 60%  $n=6$  ( $A_{1g}$  mode with  $\omega=1362$   $\text{cm}^{-1}$  and  $E_2$  mode with  $\omega=1581$   $\text{cm}^{-1}$ ) and about 20%  $n=7$  ( $E_2$  nearly degenerate with the  $E_2$  mode for  $n=5$ ).

In the Raman spectra, shown in the insets, the bands are peaked at about 1550  $\text{cm}^{-1}$ , and one may conclude that as a result of the implantation, differently termed carbon cluster rings are formed.

In the IR spectra of the samples, implanted in a PP substrate along with the bands at 1350 and 1550  $\text{cm}^{-1}$ , a band at 1450  $\text{cm}^{-1}$ , which became more pronounced with increased implantation dose, is seen. In the framework of the Doyle and Dennison consideration, the latter can be attributed to the infrared active  $B_{1u}$  (1455  $\text{cm}^{-1}$ ) and  $E_{2g}$  (1010  $\text{cm}^{-1}$ , 1569  $\text{cm}^{-1}$ ) vibrations of 6-membered rings. In confirmation, a feature, although of low intensity, can be noticed at 1010  $\text{cm}^{-1}$ . One can speculate that the 6-membered rings predominate in the implanted PP substrates, and their quantity increases with the implantation dose. A reasonable explanation of the finding is an enlargement of the graphite-like inclusions on the increased implanted dose, which leads to the formation of graphitic nano-crystallites.

**SiC.** A wide variety of SiC phonon band profiles are observed, depending on the growth conditions. The frequencies of the transverse optical (TO) phonons for the different *polytypes* in which the material crystallize are close, and lie in the range 766 – 780  $\text{cm}^{-1}$  [15]. Thus, the feature at 780  $\text{cm}^{-1}$  in the spectrum of the implanted PMMA sample can be related to the SiC fundamental phonon absorption. The noticeable feature at 740  $\text{cm}^{-1}$  in Fig. 1, as well as that at about 850  $\text{cm}^{-1}$ , may be due to morphological factors as grains of different sizes and shapes, as well as to plasmon-phonon coupling [16]. A possible explanation of the increased absorption at 1650 – 1700  $\text{cm}^{-1}$  is the two-phonon SiC one. It is worth mentioning also that the behaviour of the spectra of the implanted PP samples in the range 900 – 1250  $\text{cm}^{-1}$ , Fig. 2, is very similar to that of polycarbosilane (PCS), heated at 873 K [16].

**Si.** It is well known that although optical phonons in covalent semiconductors, and Si in particular, are not infrared active, these semiconductors absorb infrared radiation. The absorption is interpreted as a multiphonon one [17]. The most intense peaks in the experimental absorption spectra of Si are observed at 600 – 610  $\text{cm}^{-1}$  and at about 1100  $\text{cm}^{-1}$  [18]. Less intense two-phonon absorption is detected also, at about 700 and 850  $\text{cm}^{-1}$  [18]. Low intensity features at 610 and 1080  $\text{cm}^{-1}$  in the spectrum of the implanted PMMA sample, marked with arrows in Fig. 1, then can be attributed to the absorption of unreacted Si atoms. As concerns the PP samples, the presence of Si is questionable.

## 5. Conclusions

The unambiguous statement that follows from the investigation is that the implantation of Si into PP and PMMA leads to the formation of amorphous and nanocrystalline graphite, predominating in the PP substrates. The presence of SiC particles and unreacted Si atoms also looks possible.

## Acknowledgements

This work has been supported by an International Atomic Energy Agency project (No:1294/RBF). The support of Forschungs-zentrum Dresden-Rossendorf e.V., Germany, is also gratefully acknowledged.

## References

- [1] G. Marletta, in *Materials and Processes for Surface and Interface Engineering*, Kluwer Academic Publishers, Dordrecht, 597, 1995..
- [2] T. G. Vargo, J. A. Gardella, R. L. Schmitt, K. J. Hook, T. J. Hook, in *Surface Characterization of Advanced Polymers*, eds. L. Sabbattini and P. G. Zambonin, VCH Publ. Co., Weinheim, 163, 1993.
- [3] S. Balabanov, K. Krezhov, *J. Phys. D: Applied Physics* **32**, 2573 (1999).
- [4] A. Toth, T. Bell, I. Bertoti, M. Mohai, B. Zelei, *Nucl. Instrum. & Meth. B* **148**, 1131 (1999).
- [5] A. L. Evelyn, D. Ila, R. L. Zimmerman, K. Bhat, D. B. Poker, D. K. Hensley, C. Klatt, S. Kalbitzer, N. Just, C. Drevet, *Nucl. Instrum. & Meth. B* **148**, 1131 (1999).
- [6] A. L. Stepanov, *J. Techn. Phys.* **74**, 1 (2004).
- [7] L. H. Sloof, A. van Blaaderen, A. Polman, G. A. Hebbink, S. I. Klink, F. C. J. M. van Veggel, J. W. Hofstraat, *Appl. Phys. Lett.* **91**, 3955 (2002).
- [8] J. Zuk, T. Tsvetkova, S. Balabanov, E. Borisova, L. Avramov, L. Bischoff, *Vacuum*, in press.
- [9] T. Tsvetkova, S. Balabanov, L. Avramov, E. Borisova, S. Sinning, L. Bischoff, *Vacuum*, in press 2008.
- [10] T. Tsvetkova, S. Balabanov, L. Avramov, E. Borisova, I. Angelov, L. Bischoff, *Vacuum*, in press.
- [11] H. Lim, Y. Lee, S. Han, J. Cho, K. Kim, *J. Vac. Technol. A* **19**, 1490 (2001).
- [12] R. J. Collins, H. Y. Fan, *Phys. Rev.* **93**, 265 (1955).
- [13] E. György, I. Mihailescu, M. Baleva, M. Abrashev, E. P. Trifonova, A. Szekeres, A. Perrone, *Mat. Sci. & Eng. B* **97**, 251 (2003).
- [14] T. E. Doyle, J. R. Dennison, *Phys. Rev. B* **51**, 196 (1995).
- [15] J. A. Freitas, Jr., in *Properties of Silicon Carbide*, ed. G. L. Harris, EMIS Data Reviews Series, No. **13**, 29 (1995).
- [16] H. Mutschke, A. C. Andersen, D. Clement, Th. Henning, G. Peiter, *Astron. Astrophys.* **345**, 187 (1999).
- [17] M. Lax, E. Burstein, *Phys. Rev.* **97**, 39 (1955).
- [18] N. Nakayama, Y. Tsuehiya, S. Tamada, K. Kosuge, S. Nagata, K. Tahakiro, S. Yamaguchi, *Jap. J. Appl. Phys. Lett.* **32**, L1465 (1993).

\*Corresponding author: Tania\_Tsvetkova@yahoo.co.uk